RESEARCH

CrossMark

Formulation and mechanical characterization of a semi-crystalline nano-fluorine hydroxyapatite-filled dental adhesive

Kiana Shekofteh[1] · Alireza Boruziniat[1,2] · Mohammad-Javad Moghaddas[1,2] · Fatemeh Namdar[1,2] · Ehsan Zahabi[1] · Hossein Bagheri[1,2]

Abstract

The aim of this in vitro study was to evaluate the effect of adding nano-crystalline fluorine hydroxyapatite (FHAp) bioceramic into dental adhesive on the mechanical properties and bonding strength to dentin substrate. FHAp was synthesized using a sol–gel method and characterized using x-ray diffraction (XRD), Fourier transform infrared spectroscopy (FTIR), and scanning electron microscopy (SEM). Citric acid was used as the coupling agent. The fillers were added to an ethanol-based experimental dental adhesive containing Bis-GMA, TEGDMA, and HEMA (weight ratio 2:1:1). Camphorquinone (0.1%w) and ethyl-4-dimethylaminobenzoat (0.1%w) were used as photo-initiator and co-initiator for photo-polymerization at the weight ratios of 0, 0.2, 0.5, 1, and 2%. Flexural strength and modulus of photo-polymerized specimens were measured using a three-point bending test ($n = 10$ for each group). Degree of conversion (DC) was measured using FTIR. Microtensile bond strength test (µTBS) to bovine dentin was measured ($n = 10$ for each group). The data were analyzed using one-way ANOVA and Tukey post hoc tests ($\alpha = 0.05$). Results showed that the maximum flexural strength and modulus were obtained by adding 0.2 and 1% FHAp, respectively. Therefore, the FHAp fillers made the adhesive stiffer but more brittle up to 1% w/w. Adding 2% fillers decreased the mechanical properties and precipitation of some fractions of fillers was observed. The SEM imaging showed an integrated interface between fillers and the resin matrix. Moreover, the DC was not affected by the filler content and all samples showed more than 98% of conversion. Maximum µTBS was obtained in 1%-filled specimen. In conclusion, adding 1% w/w FHAp bioceramic fillers may improve the bonding strength to the dentin substrate. More studies are needed to evaluate the bioactivity of FHAp-filled dental adhesives.

Keywords Fluorine hydroxyapatite · Dental adhesive · Dental caries

Introduction

Tooth-colored restorations are spreading due to the increasing esthetic demands as well as legal restrictions in the application of other restorative materials such as dental amalgam. The failure rate of composite restorations was reported two times more than amalgam restorations [1]. Studies showed that the main challenge in the higher rate of failure in composite restorations is

recurrent carries in the restoration–tooth interface [2, 3]. One of the major problems for the use of resin composites for direct restorations is the lack of a durable and effective dentin adhesion, which may lead to marginal microleakage [4], followed by the occurrence of secondary carries [5].

The dental plaque biofilm and its deteriorative effect on the margins of restorations cannot be eliminated. However, it may be possible to reduce its effect by engineering and formulation of novel dentin adhesives, having anticariogenic properties [6]. One strategy is the use of antibacterial agents or monomers in formulation of dental adhesives [7–11]. The other one is to break the demineralization–remineralization cycle in the benefit of remineralization, by adding fluoride-releasing or other calcium-releasing bioactive components into the adhesive formulation [12–18].

Among the bioactive materials, hydroxyapatite is of interest, because it is the main inorganic component of dentin and

✉ Hossein Bagheri
Bagherih@mums.ac.ir

[1] Dental Materials Research Center, Mashhad University of Medical Sciences, Mashhad, Iran

[2] Department of Operative Dentistry, School of Dentistry, Mashhad University of Medical Sciences, Mashhad, Iran

enamel and releases calcium ions in acidic conditions [13, 14]. Hydroxyapatite has already been used as filler in experimental dental adhesives [13, 14]. On the other hand, nano-crystalline fluorine-substituted hydroxyapatite has been taken into consideration for biomedical applications [19], including enamel remineralization [20]. Considering the inhibitory role of fluoride in dental caries, the aim of this in vitro study was to evaluate the effect of adding nano-crystalline fluorine hydroxyapatite (FHAp) into an experimental dental adhesive on the mechanical properties and bond strength to dentin substrate.

Methods and materials

Preparation and characterization of ceramic filler particles

Fluorine hydroxyapatite was synthesized using a sol–gel method. Ammonium dihydrogen phosphate ($(NH_4)H_2PO_4$), calcium nitrate tetrahydrate ($CaNO_3, 4H_2O$), and sodium fluoride were used as the calcium, phosphate, and fluorine ion sources. All materials were purchased from Merck (Darmstadt, Germany). Sodium fluoride was added to phosphate solution to obtain molar ratio of P/F = 6. This solution was added to the calcium nitrate tetrahydrate solution dropwise (pH = 10–11) under vigorous stirring to achieve the final concentrations of $[Ca^{+2}] = 0.3$ M, $[PO_4^{-3}] = 0.18$ M, and $[F^-] = 0.03$ M. The pH of solution was monitored using a pH electrode (WTW SenTix 97 T probe) and adjusted in the mentioned range using 1 M sodium hydroxide solution. The precipitated gel was aged overnight while stirring and the powder was produced by centrifuging, washing by deionized distilled water for three times and air-drying. Finally, the powder was calcinated in an electrical furnace at 450 °C for 30 min at the rate of 10°/min.

The synthesized ceramic was characterized by x-ray diffraction (XRD), Fourier transform infrared spectroscopy (FTIR), and scanning electron microscopy (SEM).

XRD (X' Pert PW 3040/60, Philips, The Netherlands) was used to characterize the crystalline structure of synthesized ceramic powder. The mean size of crystallites (D) and the fraction of crystalline phase (X_c) of the synthesized particles were calculated from the XRD pattern as described previously in the literature [21]. For the mean crystalline size, the line-broadening measurement of (211) line was used in the Scherrer equation (Eq. 1):

$$D = \frac{0.89\lambda}{\beta Cos\theta} \tag{1}$$

where λ is the wavelength (CuKα), β the full width at half-maximum of the fluorine hydroxyapatite (211) line, and θ the

diffraction angle. X_c of the FHA powders was estimated using the following equation (Eq. 2):

$$B_{002} \sqrt[3]{X_c} = K \tag{2}$$

where K is a constant equal to 0.24 for variety of different hydroxyapatite powders and B_{002} is FWHM (°) of (002) line.

The powder was examined by Fourier transform infrared (FTIR) spectroscopy (Perkin Elmer Spectrum2, Singapore) using KBr method. The sample was analyzed in the range of 400–4000 cm^{-1} at a scan speed of 23 scan/min with 4 cm^{-1} resolution.

### Formulation and characterization of experimental dental adhesive

Surface treatment of FHA fillers Two grams of FHAp powder was added to 500 cm^3 of 0.2 M citric acid solution and stirred for 48 h on a magnetic stirrer hot plate (80 °C) to complete the reaction. The powder was extracted by centrifuging and air-drying at room temperature. The reaction of citric acid with the filler surface was confirmed using FTIR as above mentioned. The morphology of treated fillers was studied using SEM. An ethanol-based dental adhesive was formulated by blending bisphenol A-glycidyl methacrylate (Bis-GMA), triethyleneglycol dimethacrylate (TEGDMA), and 2-hydroxyethyl methacrylate (HEMA) (weight ratio 2:1:1). Camphorquinone (0.1%w) and ethyl-4-dimethylaminobenzoat (0.1%w) were used as photo-initiator and co-initiator for photo-polymerization. Ethanol was added just before the experiments to prevent evaporation. Fillers were added to the adhesive at the weight ratios of 0, 0.2, 0.5, 1, and 2% and dispersed using an ultrasonic bath for 2 h. All materials were purchased from Merck (Darmstadt, Germany).

Flexural strength test Flexural strength (FS) and flexural modulus (FM) were measured according to ISO 4049 [22] and ASTM D790-17 [23], respectively. Ten bar-shaped specimens (2 × 2 × 25 mm) of each adhesive were prepared using a silicon mold having the same dimensions and photo-polymerized using a LED light-curing unit (Bluephase, Ivoclar Vivadent) for 60 s in three overlapping regions. The opposite surface was also photo-polymerized as described to ensure adequate polymerization. Flexural strength test was evaluated using a three-point bending method by a universal testing machine (STM20, SANTAM, Iran) using a crosshead speed of 0.5 mm/min. FS and FM were calculated using the following formulas, respectively [22, 23]:

$$FS = \frac{3Fl}{2bh^2} \tag{3}$$

$$FM = \frac{F.l^3}{4bh^3 d} \tag{4}$$

Fig. 1 X-ray diffraction pattern of synthesized ceramic
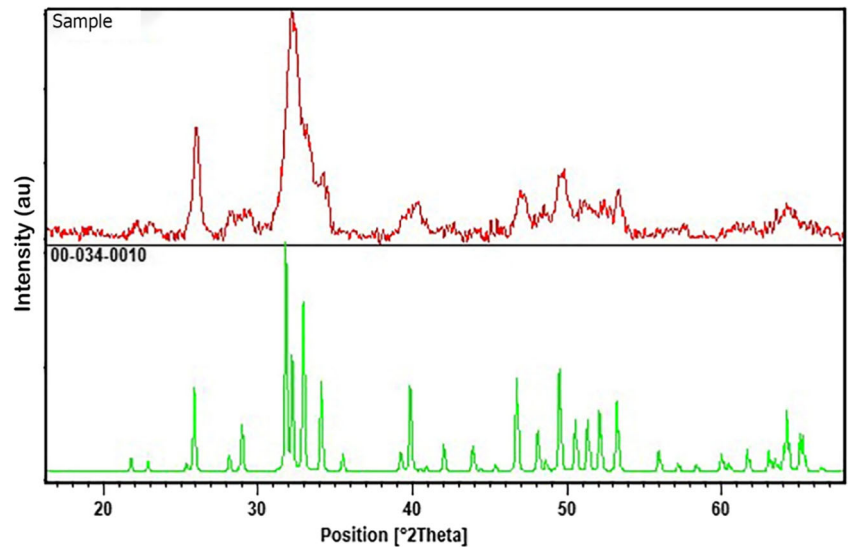
where F is the recorded force at fracture, l is the distance between the supports (20 mm), b is the width (2 mm) and h is the height (2 mm), and d is the deflection due to force F.

The mean values for flexural strength and modulus were calculated for each group and compared using one-way ANOVA, followed by Tukey's post hoc test ($\alpha = 0.05$).

Degree of conversion The infrared spectra of uncured and cured samples for each adhesive were analyzed using an FTIR spectrometer (Perkin Elmer Spectrum2, Singapore) operating at 16 scans at 4 cm^{-1} resolution. The range from 400 to 4000 cm^{-1} was scanned and the region from 1590 to 1660 cm^{-1} was expanded. The degree of conversion (DC) of each specimen was determined by comparison of the ratio of the aliphatic carbon–carbon double bond (C=C) (the peak

around 1638 cm^{-1}) to the aromatic component (around 1608 cm^{-1}) as the internal standard for the cured and uncured samples. DC of adhesive resin was calculated by the following equation [24]:

$$DC\% = 1 - \frac{C = C \text{ Aliphatic}/C = C \text{ Aromatic in polymer}}{C = C \text{ Aliphatic}/C = C \text{ Aromatic in monomer}} \times 100$$

Scanning electron microscopy The dispersion and the integrity of filler particles to the resin matrix were observed using SEM (Leo 1450VP, Zeiss, Germany). For sample preparation, the polymerized specimens were immersed in liquid nitrogen and fractured to achieve a clean surface. The fresh surface was gold sputtered and moved to the SEM chamber.

Fig. 2 FTIR spectra of FHAp and acid citric-treated FHAp. The appearance of new peaks at 1603 and 1596 corresponding to (O–C=O) group and distortion of 1033 cm^{-1} peak in FHAp indicated the reaction between FHAp particles and citric acid
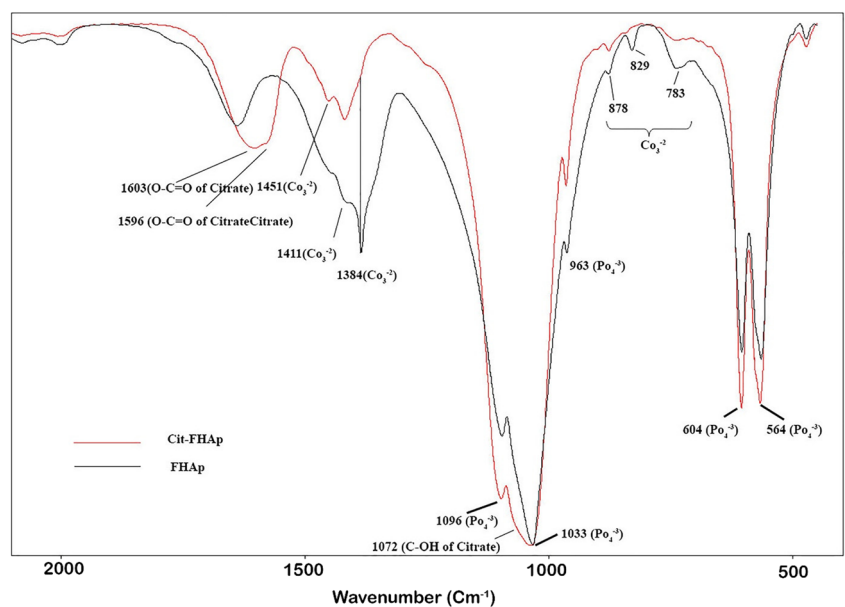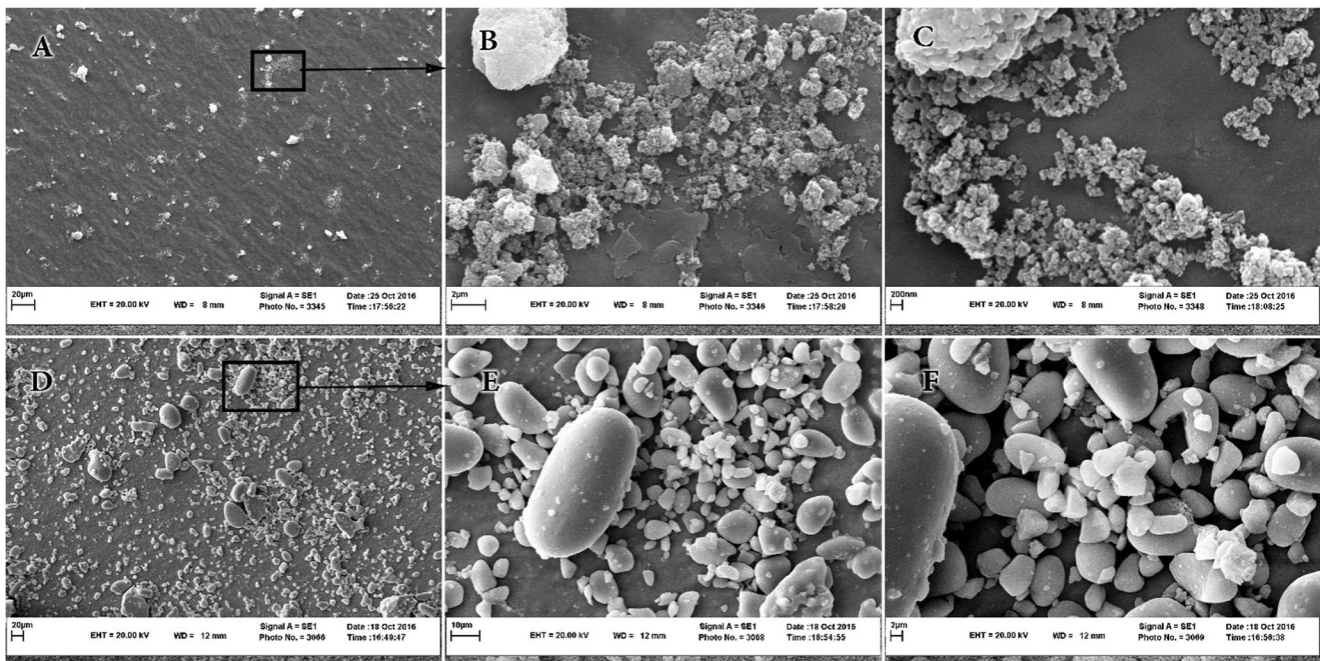
Fig. 3 SEM images of synthesized ceramic powder, representing the ceramic particles composed of agglomerated nanoparticles (**a** × 1000, **b** × 5000, **c** × 15000). After treatment by citric acid, microfillers are formed, in the range of 5 μm (**d** × 500, **e** × 2500, **f** × 5000)

Bond strength to dentin A microtensile bond strength test (μTBS) was planned to evaluate if the addition of different amounts of filler affect the bond strength of adhesive to the dentin. Bovine incisors were gathered, debrided, and disinfected in 0.1% thymol solution for 1 week. The enamel on the buccal surface was grinded using SiC sandpapers, and the exposed dentine was prepared using 600 grit SiC sandpaper to produce similar smear layer for all specimens. The working surfaces were acid-etched using 37% phosphoric acid (Denfil; Vericom Co., Korea) for 15 s and rinsed with distilled water for 10 s, and the excess water was removed using gentle airflow. The adhesive was applied on the dentine surface in three layers, each layer air-dried gently using dental air syringe after 20 s and finally photo-polymerized by a LED light-curing unit (Bluephase, Ivoclar Vivadent) for 20 s. A commercially available dental resin composite (Z250, 3M/ESPE) was bonded to the dentin surface (4 mm height) in 2-mm increments, and each increment was photo-cured for 40 s as mentioned above. The specimens were sectioned using a low-speed micro-saw

(Nemo, Mashhad, Iran) to obtain ten beams with cross-section area of approximately 1 mm^2. The specimens were attached to a universal testing machine (STM20-SANTAM, IRAN) jig for μTBS using cyanoacrylate glue, and the bond strength was measured using a 6 Kgf load-cell with a crosshead speed of 0.5 mm/min. The stress at failure point was recorded, and the mean values for μTBS were compared using one-way ANOVA followed by Tukey's post hoc test ($\alpha = 0.05$). The failure modes were determined at × 40 magnification using a stereomicroscope and recorded as adhesive, cohesive in dentin, or composite and mixed.

Results

Characterization of synthesized filler

X-ray diffraction The XRD pattern of produced powder is presented in Fig. 1 and matched with the hydroxyfluoroapatite

Table 1 Descriptive results for flexural strength

Filler content (w/w %)	Mean (MPa)	Std. deviation (MPa)	95% confidence interval for mean	
			Lower bound	Upper bound
0	31.7156	1.57641	30.5038	32.9273
0.2	37.6411	2.42481	35.7772	39.5050
0.5	34.7360	3.21121	32.4388	37.0332
1	29.8218	5.26887	26.2821	33.3615
2	27.5060	6.05753	23.1727	31.8393

Table 2 Descriptive results for flexural modulus

Filler content (w/w %)	Mean (MPa)	Std. deviation (MPa)	95% confidence interval for mean	
			Lower bound	Upper bound
0	347.9089	88.55979	279.8358	415.9820
0.2	386.8967	75.28793	329.0252	444.7681
0.5	425.9560	49.07202	390.8520	461.0600
1	512.0760	98.02434	441.9536	582.1984
2	376.5050	71.77430	325.1608	427.8492

(PDF No. 00-034-0010). Merging of (112) and (211) peaks is an indication for the formation of fluorinated hydroxyapatite [25]. Moreover, the broadening pattern indicated the formation of nano-scaled fluorine hydroxyapatite according to the Eq. 1; the mean crystalline size was calculated about 15 nm. The degree of crystallinity of powder approximated to be about 56% according to Eq. 2.

FTIR In FTIR spectrum (Fig. 2), bands located at 1095, 1032, and 962 cm^{-1} were obtained (P–O bonds), as well as in the low wavenumber region at 604 and 564 cm^{-1} (O–P–O bonds) which corresponds to the apatite structure. Furthermore, two distinctive peaks observed at 3571 and 632 cm^{-1} were assigned to the stretching mode and the vibrational mode of the structural hydroxyl anion (OH^-) in HAp, respectively [26]. Bands corresponding to the CO_3^{2-} groups were also detected. The bands at 878 and 738 cm^{-1} represent the bending and the vibration mode of C–O bond in carbonate group that partially occupying OH^- positions (A-type), while the bands detected at 1456 and 1413 cm^{-1} reflect partial PO_4^{3-} substitution (B-type) [26].

After treatment of FHAp particles by citric acid, two peaks appeared at the 1603 and 1596 cm^{-1}, corresponding to the O–C=O in citrate structure, indicating the reaction of citric acid and the surface of fillers. Furthermore, the distortion of peak at 1033 cm^{-1} in FHAp spectrum can be due to the appearance of the peak at 1072 cm^{-1}, which corresponds to the C–OH in citrate structure.

Scanning electron microscopy SEM micrographs (Fig. 3) showed the formation of microparticles, made up of agglomeration of FHAp nanoparticles. By citric acid treatment, rounded microparticles were observed in the range of 5 μm.

Characterization of the adhesive

Flexural strength and modulus The mean and standard deviation for flexural strength and modulus in each group are presented in Tables 1 and 2. One-way ANOVA showed that there is a significant difference among the mean flexural strength and modulus in different groups ($p < 0.001$ for both). The results of Tukey's post hoc analysis are shown in Fig. 4.

Degree of conversion FTIR spectra of all specimens showed that the peak at 1638 cm^{-1}, corresponding to the aliphatic C=C bond was disappeared. It indicated that the degree of
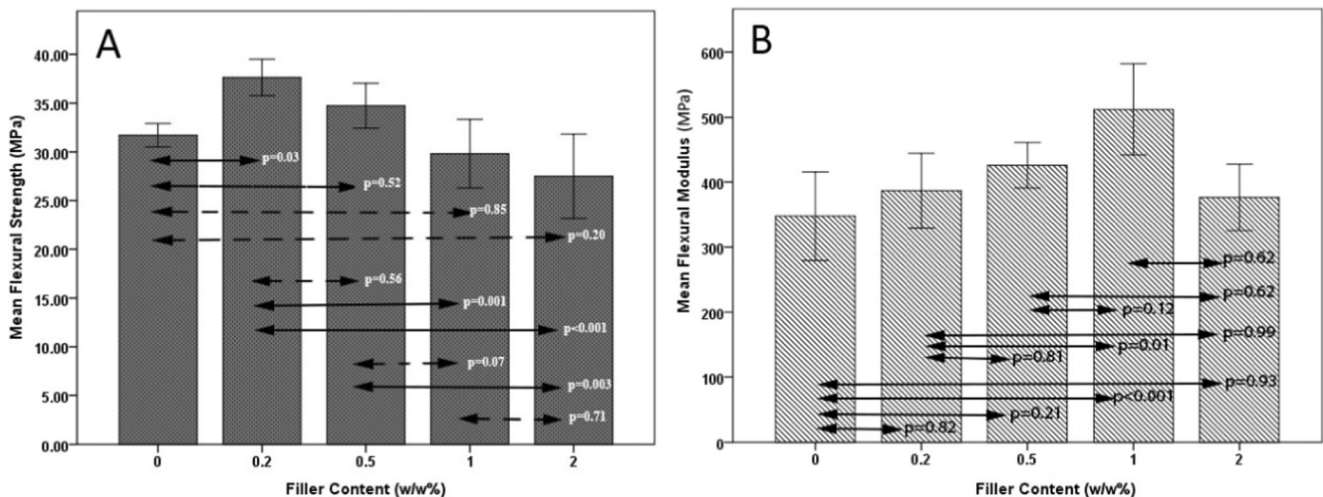

Fig. 4 Flexural strength (**a**) and flexural modulus (**b**) in different groups. Results of multiple comparison analysis (Tukey) are shown as arrows connecting each pair, and the p values are presented in front of each line.

Solid and dotted arrows are indicating significant and insignificant difference, respectively. Error bars indicate the 95% confidence intervals
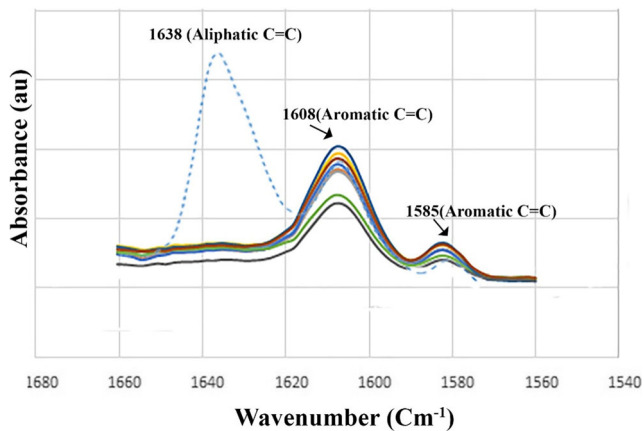
Fig. 5 FTIR spectra of adhesives in different groups. The dotted line corresponds to the uncured adhesive, while solid lines are indicating the cured adhesive specimens

conversion in all specimens was more than 98% (Fig. 5). Therefore, all specimens showed almost complete polymerization regardless of the filler content.

Microtensile bond strength Descriptive data for microtensile bond strength are shown in Table 3. One-way ANOVA showed a significant effect of filler content on the μTBS ($p = 0.001$). The results of Tukey's post hoc analysis are presented in Fig. 6.

Scanning electron microscopy SEM micrographs from fractured surface showed an integrated interface between filler particles and resin matrix, which confirms the adhesion of citric acid–treated particles to the resin. The filler particles well blocked the crack propagation throughout the resin matrix (Fig. 7).

Discussion

This study showed that the incorporation of fluorine hydroxyapatite microfillers significantly affects the mechanical properties and the bond strength to dentin substrate. FHAp fillers were synthesized by sol–gel approach, which is an easy and well-controlled method that described previously [27, 28].

XRD analysis showed that the calculated crystal size was in nano-metric scale, which was confirmed by SEM. On the other hand, SEM micrographs showed that the nanoparticles aggregated and formed microparticles, which can be due to the high surface energy of nanoparticles.

In the present study, citric acid was used for surface treatment of FHAp particles for integration of filler to the resin matrix. Citrate ions have more affinity for calcium ions than phosphate and go under ionic exchange by phosphate ions in the solid–solution interface [29]. Citric acid has been described as a favorable coupling agent for hydroxyapatite-filled di-methacrylate resin composites [30, 31]. Results of current study confirmed that citric acid well coated the particles and integrated with the resin matrix, using the FTIR and SEM.

In this study, the percentage of filler loading was chosen according to the study of Sadat-shojaei et al. in 2010 [14], in which the hydroxyapatite nanorods was used as the filler in a dental adhesive. All formulations remained stable during the period of the this study for 3 months at 4 °C, except for the adhesive having 2% w/w filler, in which some part of filler content was precipitated.

Flexural strength and modulus were measured to confirm the interaction of filler and the matrix, and it was shown that the maximum flexural strength was observed by 0.2–0.5% incorporation of FHAp fillers after which was dropped by increasing the filler content. However, maximum flexural modulus was seen in 1% (w/w) filler content. It means that in adding more FHAp fillers, the stiffness was increased; however, the strength was decreased due to the increase in brittleness. The sudden drop in FM by adding 2% w/w filler may be due to the agglomeration of particles. This was in agreement with the Sadat-shojaei's study [14]. Previously, it was demonstrated that the decrease in mechanical strength can be due to the lower degree of polymerization, as the increase of filler content may prevent the light penetration through the resin during the photo-polymerization. However, the measurement of degree of conversion using FTIR in this study showed that the polymerization was not affected by the percentage of filler content.

Table 3 Descriptive data for microtensile bond strength test

Filler content (w/w %)	Mean (MPa)	Std. deviation (MPa)	95% confidence interval for mean		Minimum	Maximum
			Lower bound	Upper bound		
0	11.3714	4.80126	6.9310	15.8119	5.20	17.25
0.2	13.4782	3.60498	11.0563	15.9000	7.02	17.20
0.5	13.8489	4.59128	10.3197	17.3781	7.66	23.06
1	21.6692	6.04444	17.0231	26.3154	11.78	31.15
2	16.9367	5.32997	12.8397	21.0336	8.14	26.27

Fig. 6 Results of Tukey's post hoc analysis for microtensile bond strength test. Error bars are indicating the 95% CI. Solid and dotted arrows show significant and insignificant difference between each two groups, respectively
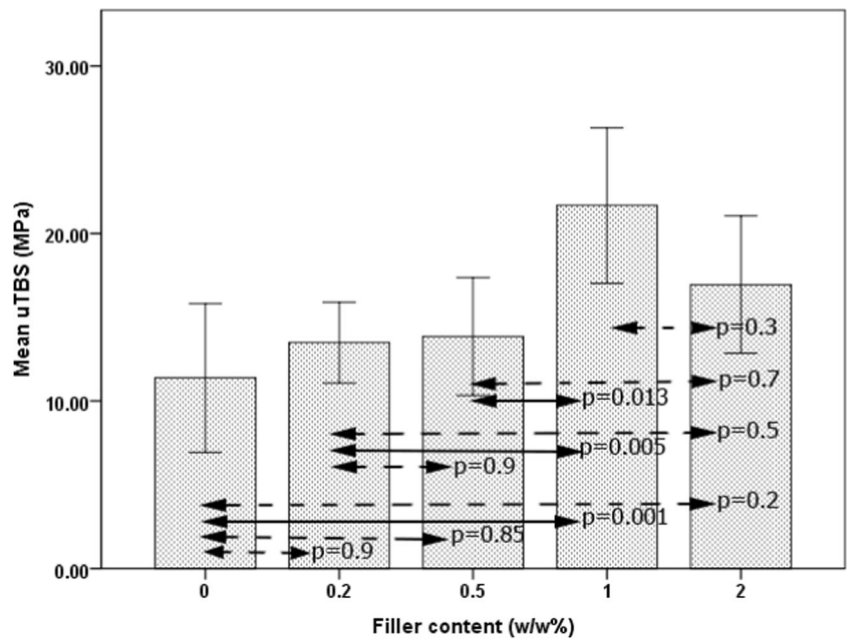
SEM showed that the filler particles act as the crack-stoppers as the failure in bending occurs due to the tensile stresses. On the other hand, the failure in bending initiates from the surface flaws that concentrate the stress. Therefore, it can be supposed that by increasing the filler content, the probability of stress concentration increases at the surface, so that the flexural strength was dropped immediately after 0.2% w/w of filler loading.

The tensile bond strength testing was chosen to evaluate the effect of FHAp filler content on the bonding effectiveness to the dentin. In this study, the maximum μTBS was achieved using 1%-loaded adhesive. The pattern of change in μTBS was consistent with that of flexural modulus, indicating that this mode of bonding test is more relevant to the flexural modulus than the ultimate strength. In addition, the inconsistency between FS and the μTBS may be due to the different behaviors of materials in the bulk and thin film forms. Regarding the effect of adhesive thickness on the bond strength, higher filler content up to 1% may increase the viscosity of adhesive that helps to form a proper thickness of adhesive. Thin layers of resin may not polymerize efficiently due to the inhibiting effect of oxygen on the polymerization. Also, a thicker layer of adhesive might act to absorb the polymerization stress of composite, which may affect the bond strength [32].
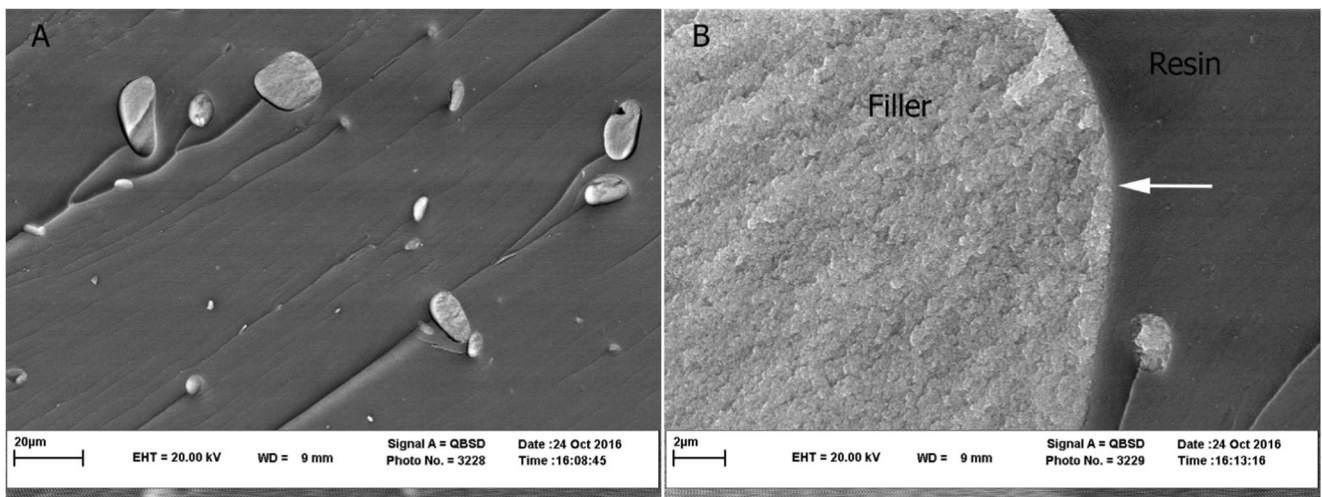

Fig. 7 SEM micrograph of 2% FHAp-filled adhesive under × 2000 (**a**) and × 15,000 magnification. The fillers stopped the crack propagation (**a**). An integrated interface was achieved between citric acid-treated FHAp particles and the resin matrix (**b**)

Conclusion

Regarding the limitations of this in vitro study, addition of 1% FHAp bioceramic particulate fillers showed an improvement in the bond strength to dentin substrate. Further study is needed to assess if the incorporation of this type of filler can inhibit the demineralization of dental substrate during pH cycling.

References

1. Ferracane, J.L.: Resin-based composite performance: are there some things we can't predict? Dent Mater. **29**(1), 51–58 (2013)
2. Opdam, N., Bronkhorst, E., Loomans, B., Huysmans, M.-C.: 12-year survival of composite vs. amalgam restorations. J Dent Res. **89**(10), 1063–1067 (2010)
3. Li, F., Weir, M.D., Fouad, A.F., Xu, H.H.: Effect of salivary pellicle on antibacterial activity of novel antibacterial dental adhesives using a dental plaque microcosm biofilm model. Dent Mater. **30**(2), 182–191 (2014)
4. Spencer, P., Ye, Q., Park, J., Topp, E.M., Misra, A., Marangos, O., et al.: Adhesive/dentin interface: the weak link in the composite restoration. Ann Biomed Eng. **38**(6), 1989–2003 (2010)
5. Donmez, N., Belli, S., Pashley, D.H., Tay, F.: Ultrastructural correlates of in vivo/in vitro bond degradation in self-etch adhesives. J Dent Res. **84**(4), 355–359 (2005)
6. Spencer, P., Ye, Q., Misra, A., SEDP, G., Laurence, J.: Proteins, pathogens, and failure at the composite-tooth interface. J Dent Res. **93**(12), 1243–1249 (2014)
7. Zhang, K., Wang, S., Zhou, X., Xu, H., Weir, M., Ge, Y., et al.: Effect of antibacterial dental adhesive on multispecies biofilms formation. J Dent Res. **94**(4), 622–629 (2015)
8. Cocco, A.R., da Rosa, W.L.D.O., da Silva, A.F., Lund, R.G., Piva, E.: A systematic review about antibacterial monomers used in dental adhesive systems: current status and further prospects. Dent Mater. **31**(11), 1345–1362 (2015)
9. Corrêa, J.M., Mori, M., Sanches, H.L., Cruz, A.D.D., Poiate, E., Poiate, I.A.V.P.: Silver nanoparticles in dental biomaterials. Int J Biomater. **2015**, (2015). https://doi.org/10.1155/2015/485275
10. Zhang, K., Li, F., Imazato, S., Cheng, L., Liu, H., Arola, D.D., et al.: Dual antibacterial agents of nano-silver and 12-methacryloyloxydodecylpyridinium bromide in dental adhesive to inhibit caries. J Biomed Mater Res B Appl Biomater. **101**(6), 929–938 (2013)
11. Zhang, N., Weir, M.D., Romberg, E., Bai, Y., Xu, H.H.: Development of novel dental adhesive with double benefits of protein-repellent and antibacterial capabilities. Dent Mater. **31**(7), 845–854 (2015)
12. Lezaja, M., Jokic, B.M., Veljovic, D.N., Miletic, V.: Shear bond strength to dentine of dental adhesives containing hydroxyapatite nano-fillers. J Adhes Sci Technol. **30**(24), 2678–2689 (2016)
13. Leitune, V.C.B., Collares, F.M., Trommer, R.M., Andrioli, D.G., Bergmann, C.P., Samuel, S.M.W.: The addition of nanostructured hydroxyapatite to an experimental adhesive resin. J Dent. **41**(4), 321–327 (2013)
14. Sadat-Shojai, M., Atai, M., Nodehi, A., Khanlar, L.N.: Hydroxyapatite nanorods as novel fillers for improving the properties of dental adhesives: synthesis and application. Dent Mater. **26**(5), 471–482 (2010)
15. Imazato, S., Ma, S., Chen, J.-H., Xu, H.H.: Therapeutic polymers for dental adhesives: loading resins with bio-active components. Dent Mater. **30**(1), 97–104 (2014)
16. Zhang, L., Weir, M.D., Hack, G., Fouad, A.F., Xu, H.H.: Rechargeable dental adhesive with calcium phosphate nanoparticles for long-term ion release. J Dent. **43**(12), 1587–1595 (2015)
17. Dionysopoulos, D., Koliniotou-Koumpia, E., Helvatzoglou-Antoniades, M., Kotsanos, N.: Fluoride release and recharge abilities of contemporary fluoride-containing restorative materials and dental adhesives. Dent Mater J. **32**(2), 296–304 (2013)
18. Dionysopoulos, D., Koliniotou-Koumpia, E., Helvatzoglou-Antoniades, M., Kotsanos, N.: In vitro inhibition of enamel demineralisation by fluoride-releasing restorative materials and dental adhesives. Oral Health Prev Dent. **14**(4), 371–380 (2016)
19. Shafiei, F., Behroozibakhsh, M., Moztarzadeh, F., Haghbin-Nazarpak, M., Tahriri, M.: Nanocrystalline fluorine-substituted hydroxyapatite [Ca 5 (PO 4) 3 (OH) 1-x F x (0≤ x≤ 1)] for biomedical applications: preparation and characterisation. IET Micro Nano Lett. **7**(2), 109–114 (2012)
20. Behroozibakhsh, M., Shafiei, F., Hooshmand, T., Moztarzadeh, F., Tahriri, M., Gorgani, H.B.: Effect of a synthetic nanocrystalline-fluorohydroxyapatite on the eroded enamel lesions. Dent Mater. **30**, e117–e1e8 (2014)
21. Sanosh, K.P., Chu, M.-C., Balakrishnan, A., Kim, T.N., Cho, S.-J.: Preparation and characterization of nano-hydroxyapatite powder using sol-gel technique. Bull Mater Sci. **32**(5), 465–470 (2009)
22. Standard I: ISO 4049 polymer based filling, restorative and luting materials. International Organization for Standardization. 2000, 1–27
23. ASTM S: Standard test methods for flexural properties of unreinforced and reinforced plastics and electrical insulating materials. ASTM D790-17. Annual book of ASTM Standards (2017)
24. Yu, P., Yap, A., Wang, X.: Degree of conversion and polymerization shrinkage of bulk-fill resin-based composites. Oper Dent. **42**(1), 82–89 (2017)
25. Moshaverinia, A., Ansari, S., Moshaverinia, M., Roohpour, N., Darr, J.A., Rehman, I.: Effects of incorporation of hydroxyapatite and fluoroapatite nanobioceramics into conventional glass ionomer cements (GIC). Acta Biomater. **4**(2), 432–440 (2008)
26. Edie, D.: The effect of processing on the structure and properties of carbon fibers. Carbon. **36**(4), 345–362 (1998)
27. Zhang, S., Xianting, Z., Yongsheng, W., Kui, C., Wenjian, W.: Adhesion strength of sol–gel derived fluoridated hydroxyapatite coatings. Surf Coat Technol. **200**(22), 6350–6354 (2006)
28. Aghbolagh, Z.S., Mahjoub, A., Ghammamy, S.: Synthesis, characterization, of fluorohydroxyapatite nanopowders by sol-gel processing. Int J Nano Dimension. **5**(3), 291 (2014)
29. López-Macipe, A., Gómez-Morales, J., Rodriguez-Clemente, R.: The role of pH in the adsorption of citrate ions on hydroxyapatite. J Colloid Interface Sci. **200**(1), 114–120 (1998)
30. Domingo, C., Arcis, R., Osorio, E., Osorio, R., Fanovich, M.A., Rodriguez-Clemente, R., et al.: Hydrolytic stability of experimental hydroxyapatite-filled dental composite materials. Dent Mater. **19**(6), 478–486 (2003)
31. Arcis, R.W., López-Macipe, A., Toledano, M., Osorio, E., Rodriguez-Clemente, R., Murtra, J., et al.: Mechanical properties of visible light-cured resins reinforced with hydroxyapatite for dental restoration. Dent Mater. **18**(1), 49–57 (2002)
32. Choi, K., Condon, J., Ferracane, J.: The effects of adhesive thickness on polymerization contraction stress of composite. J Dent Res. **79**(3), 812–817 (2000)